Chemical Physics Letters 516 (2011) 204–207

Contents lists available at SciVerse ScienceDirect

Chemical Physics Letters

journal homepage: www.elsevier.com/locate/cplett

Intriguing hybrid nanotubes with tunable structures

Li Li [a,b], Lijie Zhang [c], Jing Ren [a], Hui Zhang [a], Xuemei Sun [a], Houpu Li [a], Tao Chen [a], Huisheng Peng [a,*]

[a] Key Laboratory of Molecular Engineering of Polymers of Ministry of Education, Department of Macromolecular Science, Laboratory of Advanced Materials, Fudan University, Shanghai 200438, China
[b] College of Food Science and Technology, Shanghai Ocean University, Shanghai 201306, China
[c] State Key Lab of Silicon Materials, Zhejiang University, Hangzhou 310027, China

ARTICLE INFO

Article history:
Received 10 August 2011
In final form 30 September 2011
Available online 6 October 2011

ABSTRACT

Novel hybrid nanomaterials with iron oxide nanoparticles incorporated in nitrogen-doped carbon nanotube have been synthesized with tunable structures by a ready chemical vapor deposition process. These hybrid nanotubes show promising electronic applications.

1. Introduction

Carbon nanotubes have been extensively investigated for a wide variety of applications due to their unique structures which provide them intriguing chemical and physical performances [1–4], e.g., excellent electronic properties [5–8]. In order to further improve their electronic properties, other components have been introduced through two typical approaches. For the first approach, other elements such as N, P, and B, have been chemically doped into carbon lattices [9,10]. For the second approach, the other moieties, mainly metal, metal oxide, and C60, are physically filled into hollow parts [11,12]. To the best of our knowledge, few studies have been available to combine the above two approaches to achieve better performances. Herein, we have simultaneously realized chemical doping of nitrogen and physical filling of iron oxide nanoparticles through a ready chemical vapor deposition process (Figure S1). The resulting hybrid nanotubes exhibit tunable structures which enable controlled and remarkable electronic properties. Lithium ion battery, as an application example, has been investigated with high performance.

2. Experimental section

Hybrid nanotube arrays were synthesized by a chemical vapor deposition in a quartz tube furnace using Fe (1 nm)/Al_2O_3 (10 nm) on silicon wafer as the catalyst, ethylenediamine as both carbon and nitrogen sources, a mixture of Ar (560 sccm) and H_2 (40 sccm) gases as carrying gas. The experimental setup is shown in Figure S1, and the reaction was typically performed at 790 °C for 15 min. The structures of nanotubes were characterized by transmission electron microscopy (TEM, JEOL JEM-2100F operated at 200 kV) and scanning electron microscopy (SEM, Hitachi FE-SEM S-4800 operated at 1 kV). TEM samples were prepared by drop-casting *N*,*N*-dimethyl formamide solutions of nanotubes onto copper grids in the open air. X-ray photoemission spectroscopy was carried out on a RBD upgraded PHI-5000C ESCA system. Electrical resistivities of nanotubes were measured by 4200-SCS (Keithley Instruments Inc.). Hybrid nanotubes were used as working electrode and a lithium metal was used as counter/reference electrode to fabricate lithium ion batteries. The fabrication and measurement details for the lithium ion batteries can be found elsewhere [13].

To make single nanotube devices, the hybrid nanotubes were first dispersed in DMF using ultrasonic agitation for 3 min. A drop of the solution was then spread onto a wafer with 500-nm-thick thermal oxidized layer. At the top of the wafer with nanotubes, a 400-nm-thick E-Beam resist layer (PMMA950K, 4%, ALLRESIST, Germany) was spin-coated at 3000 rpm. for 30 s. The gold source/drain electrodes were then defined by electron beam lithography (30 kV, 110 pA, Nanometer Pattern Generation System installed in FEI Nova Nano SEM 200, USA), followed by gold metallization using thermal evaporation (5×10^{-3} Pa, 0.5 nm s^{-1}, Bench-Top Vacuum Evaporator, Quorum Thchnologies Inc., US) and lift off. The electrical performance of the individual nanotube devices were measured by 4200-SCS (Keithley Instruments Inc.) combined with four-probe station (ST-3, The 45th Research Institute of China Electronics Technology Group Corporation) at room temperature and atmospheric pressure.

3. Results and discussion

Figure 1 shows structures of as-synthesized hybrid nanotubes characterized by scanning electron microscopy (SEM) and transmission electron microscopy (TEM). The hybrid nanotubes were prepared in form of array (see Fig. 1a), and they could be easily scaled up with high efficiency. These nanotubes are mainly grown in the direction vertical to the substrate and are highly aligned

* Corresponding author.
E-mail address: penghs@fudan.edu.cn (H. Peng).

0009-2614/$ - see front matter © 2011 Elsevier B.V. All rights reserved.
doi:10.1016/j.cplett.2011.09.077

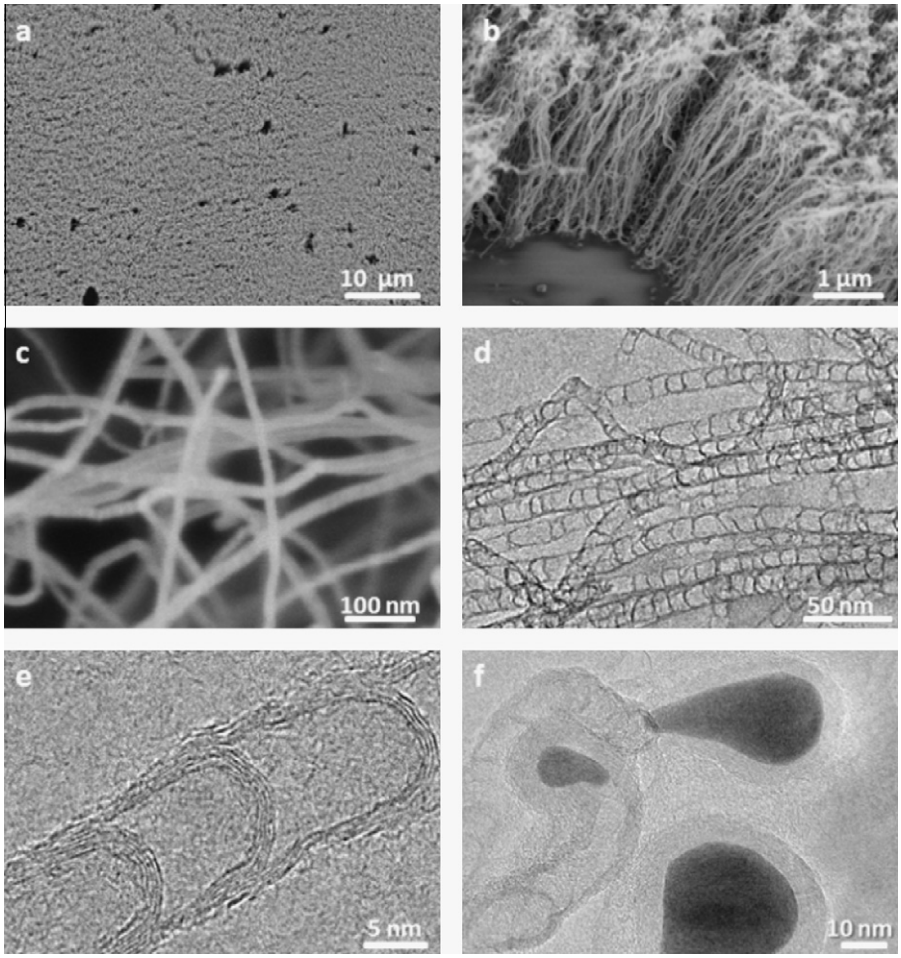

Figure 1. Scanning electron microscopy (SEM) and transmission electron microscopy (TEM) images of as-synthesized hybrid nanotubes. (a) Top view of a nanotube array by SEM. (b) Side view of a nanotube array by SEM. (c) SEM image of nanotubes at higher magnification. (d) TEM image of nanotubes. (e) High-resolution TEM image of the middle part of a nanotube. (f) High-resolution TEM image of nanotube ends.

with each other (see Fig. 1b). The nanotube lengths may be controlled from 1 to 10 μm by the varying growth time, and their diameters range from 10 to 20 nm (see Fig. 1c). TEM image (Fig. 1d) indicates a bamboo-shaped morphology for the hybrid nanotubes, similar to typical nitrogen-doped carbon nanotubes [14,15]. The structural details of bamboo can be found from high-resolution TEM image in Figure 1e. For as-synthesized nanotubes, catalytic nanoparticles with a spindle shape were observed at their close ends (see Fig. 1f), and no nanoparticles were found at their middle parts.

Elemental contents in middle parts of hybrid nanotubes were determined by energy dispersive X-ray analysis (Figure S2), and the molar ratios of C/N/Fe are calculated to be 361:16:1. In addition, nitrogen states were further analyzed by X-ray photoemission spectroscopy, and a typical graph is shown in Figure S3 with two characteristic binding energies at 400.2 and 404.1 eV. The peak at 400.2 eV corresponds to a trigonal nitrogen phase bonded to a sp2-coordinated carbon, so nitrogen atoms are successfully doped into carbon lattices. The peak at 404.1 eV further indicates that nitrogen atoms are doped in the inner carbon layers of hybrid nanotubes [16,17].

Hybrid nanotubes were stable and maintained original structures after being heated at temperatures lower than 400 °C in air. Figure 2a shows a typical TEM image of hybrid nanotubes after heating treatment of 350 °C, and bamboo structures are well retained. However, spherical nanoparticles with diameter of ~4.5 nm appear in nanotubes after heating treatment of 400 °C, and they are composed of Fe_2O_3 based on electron diffraction (see Fig. 2b) [18]. These Fe_2O_3 nanoparticles had been mainly found in compartments between two neighboring bamboos which were maintained after the above heating process. The heated nanotubes also retained good tenacity and toughness (see Figure S4). However, bamboos were destroyed to form normal linear structures after further treatment at 450 °C or higher temperatures, and Fe_2O_3 nanoparticles fuse into larger and irregular aggregates (Fig. 2c). At this point, the resulting nanotubes became brittle and easily broke. Macroscopically, hybrid nanotube arrays maintain highly aligned structures after heating treatment below 400 °C (see Fig. 2d) but form networked structures after being heated at 450 °C (see Fig. 2e). The heating treatment at higher temperatures, e.g., 500 °C, would totally destroy nanotubes.

Raman spectroscopy is useful to evaluate structure integrity of carbon-based nanotubes. Therefore, structures of hybrid nanotubes had been also traced by Raman spectroscopy during heating treatments. It is well known that two characteristic peaks of D-band and G-band arise from defects or disorder of graphene sheets and C–C stretching (E2g) model of graphite, respectively, and intensity ratio of D-band to G-band reflects crystallinity degree. Here D-band and G-band were observed at ~1355 and ~1580 cm^{-1}, respectively [19]. The intensity ratios of D-band to G-band gradually increase with increasing treatment temperatures (Fig. 2f), and they are calculated to be 0.96, 0.98, 1.01, and 1.10, for

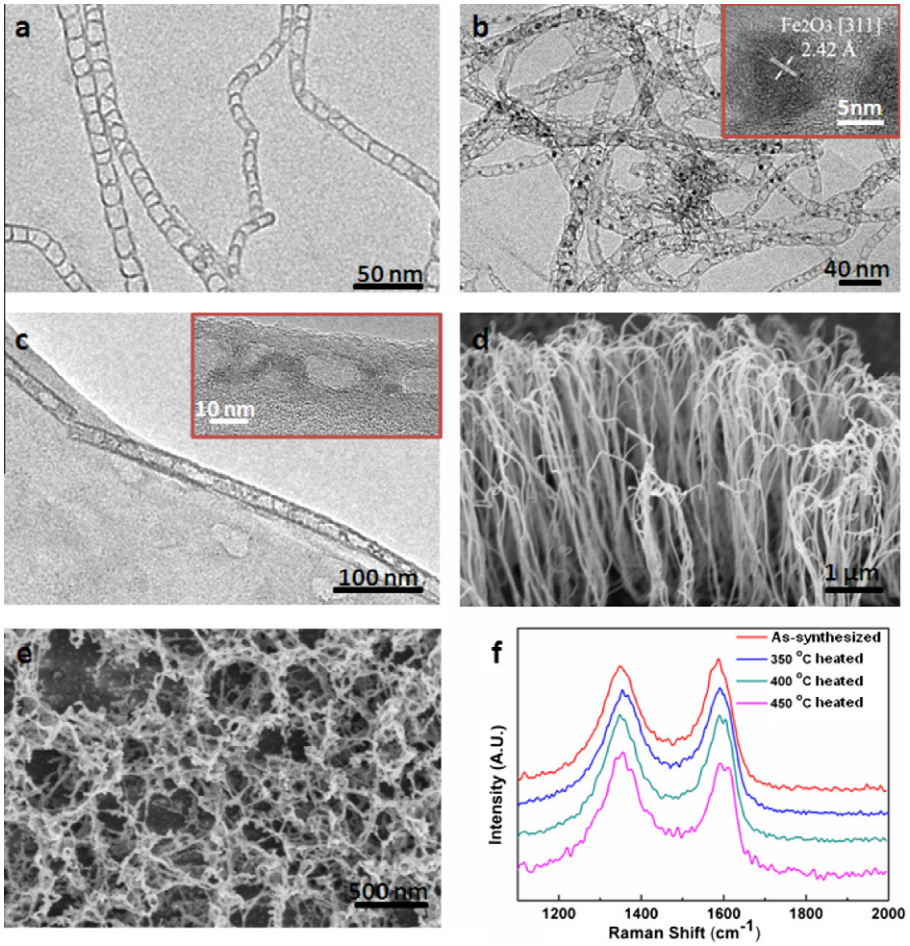

Figure 2. Hybrid nanotubes with tunable structures. (a–c) High-resolution TEM images of hybrid nanotubes after heating treatments in air at 350, 400, and 450 °C, respectively. (d and e) SEM images of hybrid nanotubes after heating treatments at 400 and 450 °C, respectively. (f) Raman spectra of as-synthesized and heated nanotubes at different temperatures.

as-synthesized and heated nanotubes at 350, 400, and 450 °C, respectively. This result agrees with TEM and SEM observations.

Electrical properties of hybrid nanotubes before and after being treated at different temperatures had been also studied by comparing their electrical resistivities (see Figure S5). The preparations of samples for electrical measurements were made according to the widely reported process [9]. For a typical test, nanotube samples were dispersed in *N*,*N*-dimethylformamide followed by coating onto SiO_2/Si substrate, and two Au electrodes were then carefully deposited to connect a nanotube to perform I–V measurements. The gold electrodes were tightly covered on the hybrid nanotube to reduce the contacting resistances. In fact, the resistances increased with increasing lengths of hybrid nanotubes, indicating that contacting resistances may be neglected in the tests. It was further found that the electrical resistivities of a hybrid nanotube increased with increasing heating temperatures as treatments at higher temperatures decreased ordered lattice structures confirmed by Raman spectra. Figure S5 shows representative I–V curves of a hybrid nanotube before and after being heated at 400 °C. Electrical resistivities are calculated to be 8.9×10^{-5} and 19.5×10^{-5} Ω cm, respectively.

Synthesis and structure evolution of these hybrid nanotubes are summarized as Figure 3. It is well known that iron film breaks to induce growth of hybrid nanotubes. During the growing process, nitrogen atoms are doped into carbon lattice to form a bamboo structure. In addition, some iron from catalytic nanoparticles may be carried away and dispersed in inner walls of

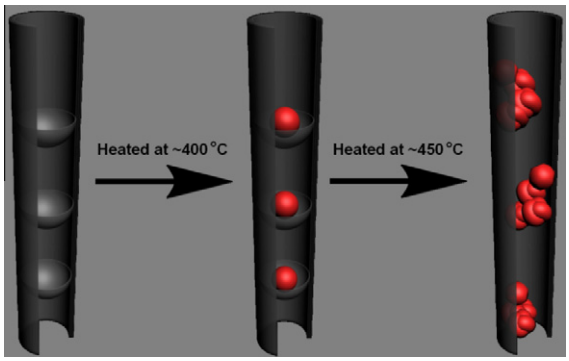

Figure 3. Schematic illustration of the structure evolution after heating treatment.

nitrogen-doped carbon nanotubes. As no nanoparticles were observed in as-synthesized hybrid nanotubes under high-resolution TEM, the dispersed iron should exist atomically or in a few atoms. After heated to equal to or higher than 400 °C, the dispersed iron may be oxidized and aggregated into nanoparticles. With further heating treatment at 450–500 °C, the bamboo structure is destroyed, and iron oxide nanoparticles fuse into larger irregular aggregates. More studies are under way.

Due to excellent electrochemical properties, carbon-based nanotubes represent an effective electrode material for lithium ion battery [20–22]. Here as-synthesized and heated hybrid

nanotubes were used as anodes to fabricate batteries, and the battery performances are compared to investigate the structure effect. Figure S6a shows typical charge/discharge profiles of a battery derived from hybrid nanotubes. Voltage profiles were almost unchanged with increasing cycles, i.e., the battery maintained stable performance. In addition, the specific capacities depend on structures of hybrid nanotubes (see Figure S6b). A battery prepared from as-synthesized nanotubes exhibits an average capacity of ~300 mAh/g. For the nanotubes after heating treatment at 350 °C, the resulting battery shows an increased average capacity of 890 mAh/g. The resulting batteries exhibit decreasing capacities with further increasing treatment temperatures, e.g., 470 mAh/g for those nanotubes heated at 400 °C. Here the battery capacities can be much higher than both graphite and nitrogen-doped or Fe_2O_3-filled carbon nanotubes [23–26].

The capacity changes are closely related to structures of hybrid nanotubes. Nitrogen doping decreases the ordered structure in carbon lattice and produces defects, which improves their electrochemical performances [23,24,27], and filling of Fe_2O_3 also improves electrochemical performances [25]. After heating treatment at 350 °C, nitrogen doping results in formation of more defects, and iron oxidizes to produce Fe_2O_3, both of which increase their electrochemical performances. With further increase of heating temperatures, the nitrogen-doping effect continues enhancing their electrochemical performances. However, iron oxide forms nanopartices or even larger irregular aggregates with decreasing interaction surface areas to greatly reduce their electrochemical performances, which exceeds the nitrogen-doping effect. Therefore, the charge capacities of derived batteries decrease. A detailed study will be provided later.

4. Conclusion

In summary, novel hybrid nanotubes with tunable structures and controlled excellent electronic properties have been synthesized by chemical vapor deposition. These nanostructures show promising applications in various electronic devices, e.g., as high-performance electrode for lithium ion battery.

Acknowledgements

This work was supported by Natural National Science Foundation of China (20904006, 91027025), Ministry of Science and Technology (2011CB932503, 2011DFA51330), Science and Technology Commission of Shanghai Municipality (1052nm01600, 09PJ1401100), Program for New Century Excellent Talents in University (NCET-09-0318), Ministry of Education of China, and Li Foundation Heritage Prize.

Appendix A. Supplementary data

Supplementary data associated with this article can be found, in the online version, at doi:10.1016/j.cplett.2011.09.077.

References

[1] L. Hu, D.S. Hecht, G. Grüner, Chem. Rev. 110 (2010) 5790.
[2] P. Diao, Z.F. Liu, Adv. Mater. 22 (2010) 1.
[3] T. Chen et al., Angew. Chem. Int. Edit. 50 (2011) 1815.
[4] Y.K. Zhou, J. Wang, Y.Y. Hu, R. ÒHayre, Z.P. Shao, Chem. Commun. 46 (2010) 7151.
[5] H. Peng, M.K. Jain, Q. Li, D.E. Peterson, Y. Zhu, Q. Jia, J. Am. Chem. Soc. 130 (2008) 1130.
[6] K.P. Gong, F. Du, Z.H. Xia, M. Durstock, L.M. Dai, Science 323 (2009) 760.
[7] Y.F. Tang, B.L. Allen, D.R. Kauffman, A. Star, J. Am. Chem. Soc. 131 (2009) 13200.
[8] W. Xiong et al., J. Am. Chem. Soc. 132 (2010) 15839.
[9] K. Xiao, Y.Q. Liu, A.P. Yu, G. Hu, Y.M. Sun, D.B. Zhu, J. Am. Chem. Soc. 127 (2005) 8614.
[10] V. Krstíc, G.L.J.A. Rikken, P. Bernier, S. Roth, M. Glerup, Europhys. Lett. 77 (2007) 37001.
[11] D. Ugarte, A. Chatelain, W.A. de Heer, Science 274 (1996) 1897.
[12] B.T. Hang, H. Hayashi, S.H. Yoon, S. Okada, J. Yamaki, J. Power Sources 178 (2008) 393.
[13] L. Li et al., Adv. Mater. 23 (2011) 3730.
[14] M. Glerup, M. Castignolles, M. Holzinger, G. Hug, A. Loiseaub, P. Berniera, Chem. Commun. 20 (2003) 2542.
[15] X. Xu, S.J. Jiang, Z. Hu, S.Q. Liu, ACS Nano 4 (2010) 4292.
[16] S. Maldonado, K.J. Stevenson, J. Phys. Chem. B 109 (2005) 4704.
[17] X.B. Wang, Y.Q. Liu, D.B. Zhu, L. Zhang, H.Z. Ma, N. Yao, B.L. Zhang, J. Phys. Chem. B 106 (2002) 2186.
[18] W. Chen, X.L. Pan, W.M. Georg, D.S. Su, X.H. Bao, J. Am. Chem. Soc. 128 (2006) 3136.
[19] S.H. Lim, H.I. Elim, X.Y. Gao, A.T.S. Wee, W. Ji, J.Y. Lee, J. Lin, Phys. Rev. B 73 (2006) 045402.
[20] H.X. Zhang, C. Feng, Y.C. Zhai, K.L. Jiang, Q.Q. Li, S.S. Fan, Adv. Mater. 21 (2009) 2299.
[21] Y.K. Zhou, J. Wang, Y.Y. Hu, R. ÓHayre, Z.P. Shao, Chem. Commun. 46 (2010) 7151.
[22] B.J. Landi, M.J. Ganter, C.D. Cress, R.A. DiLeo, R.P. Raffaelle, Energy Environ. Sci. 2 (2009) 638.
[23] V.L. Pushparaj, M.M. Shaijumon, A. Kumar, S. Murugesan, L. Ci, R. Vajtai, R.J. Linhardt, O. Nalamasu, P.M. Ajayan, Proc. Natl. Acad. Sci. USA 104 (2007) 13574.
[24] J. Chen, Y. Liu, A.I. Minett, C. Lynam, J. Wang, G.G. Wallace, Chem. Mater. 19 (2007) 3595.
[25] W.J. Yu, P.X. Hou, L.L. Zhang, F. Li, C. Liu, H.M. Cheng, Chem. Commun. 46 (2010) 8576.
[26] D.Y. Zhong, G.Y. Zhang, S. Liu, E.G. Wang, Q. Wang, H. Li, X.J. Huang, Appl. Phys. Lett. 79 (2001) 3500.
[27] K. Nishidate, M. Hasegawa, Phys. Rev. B 71 (2005) 245418.